

ORIGINAL CONTRIBUTION

OMA1 and YME1L as a Diagnostic Panel in Hepatocellular Carcinoma

Shimaa A. Abass^a, Nabil Mohie Abdel-Hamid^a, Ahmed M. Elshazly^{b,c,*}, Walied Abdo^d, and Sherin Zakaria^b

^aBiochemistry Department, Faculty of Pharmacy, Kafrelsheikh University, Kafrelsheikh, Egypt; ^bDepartment of Pharmacology and Toxicology, Faculty of Pharmacy, Kafrelsheikh University, Kafrelsheikh, Egypt; ^cDepartment of Pharmacology and Toxicology, Massey Cancer Center, Virginia Commonwealth University, Richmond, VA, USA; ^dDepartment of Pathology, Faculty of Veterinary Medicine, Kafrelsheikh University, Kafrelsheikh, Egypt

Identifying new hepatocellular carcinoma (HCC)-driven signaling molecules and discovering their molecular mechanisms are crucial for efficient and better outcomes. Recently, OMA1 and YME1L, the inner mitochondrial proteases, were displayed to be associated with tumor progression in various cancers; however, their role in HCC has not yet been studied. Therefore, we evaluated the possible role of OMA1/YME1L in HCC staging and discussed their potential role in cellular apoptosis and proliferation. Our study was performed using four groups of male albino rats: a normal control and three diethyl nitrosamine-treated groups for 8, 16, and 24 weeks. The OMA1 and YME1L, matrix-metalloproteinase-9 (MMP-9), and cyclin D1 content were measured in liver tissues, while alpha-fetoprotein (AFP) level was assessed in serum. Additionally, Ki-67 expression was evaluated by immunohistochemistry. The relative hepatic expression of Bax, and tissue inhibitor matrix metalloproteinase (TIMP-3) was measured. Herein, we confirmed for the first time that OMA1 is down-regulated while YME1L is up-regulated in HCC in the three studied stages with subsequent inhibition of apoptosis and cell cycle progression. Furthermore, these proteases have a possible role in metastasis. These newly recognized results suggested OMA1 and YME1L as possible diagnostic tools and therapeutic targets for HCC management.

INTRODUCTION

Hepatocellular carcinoma (HCC) is considered the leading cause of mortality in cirrhosis and the main cause of cancer-related death globally [1]. Patients with advanced HCC have poor overall survival. On the other

hand, the survival of early-diagnosed patients is markedly improved due to curative interventions such as ablative therapies, surgical resection, or liver transplantation [2]. Until now, the standard surveillance of HCC involves serum alpha-fetoprotein (AFP) and abdominal ultrasound with a combined sensitivity of approximately 60%. Sev-

*To whom all correspondence should be addressed: Ahmed M. Elshazly, Department of Pharmacology and Toxicology, Massey Cancer Center, Virginia Commonwealth University, Richmond, VA, USA; Email: Ahmed_elshazly@pharm.kfs.edu.eg; Elshazlyam@vcu.edu. ORCID: 0000-0003-0353-1643.

Abbreviations: AFP, alpha-fetoprotein; DENA, Diethyl nitrosamine; HCC, Hepatocellular carcinoma; IMM, inner mitochondrial membrane; GSH, reduced glutathione; MDA, malondialdehyde; MMP-9, matrix-metalloproteinase-9; NSCLC, non-small cell lung cancer; OPA1, optic atrophy 1; PB, phenobarbital sodium; TIMP-3, tissue inhibitor matrix metalloproteinase; YME1L, YME1 like 1 ATPase; ROS, reactive oxygen species; TUNEL, Terminal Deoxynucleotidyl Transferase (TdT) dUT-PNick-End Labeling.

Keywords: Hepatocellular carcinoma, OMA1, YME1L, mitochondrial proteins

Author Contributions: SZ designed the experiments and reviewed the manuscript. SAA performed the experiment and data analysis and wrote the manuscript. AME and NMA-H revised and edited the manuscript. All authors have read and agreed to the published version of the manuscript. WA performed the histopathological analysis of the study.

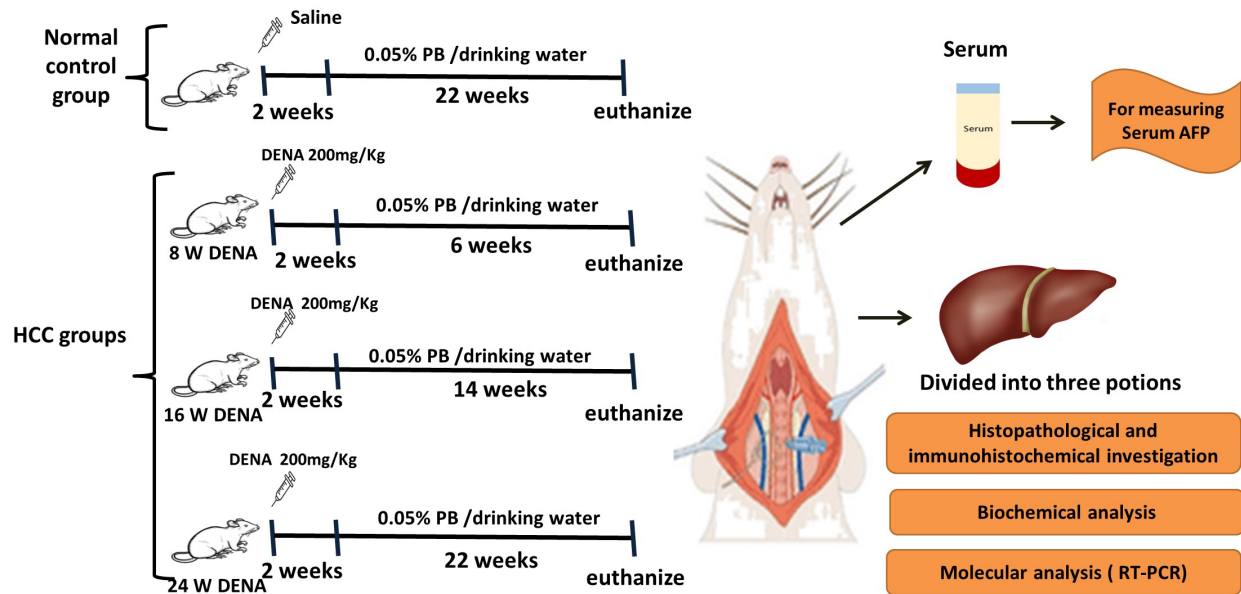


Figure 1. Schematic diagram of the experimental design. DENA: diethyl nitrosamine; PB: sodium phenobarbital; AFP: alpha feto-protein.

eral conditions contribute to the reliability of AFP, including liver disease and inflammation, which negatively affect its specificity [3]. Additionally, the abdominal ultrasound is operator-dependent and its performance may be affected by body habitus [4]. Due to the suboptimal performance of the current surveillance strategies, there is an urgent need to develop new biomarkers with more effective performance that may help in early HCC diagnosis, especially in high-risk patients, and eventually endorse timely diagnosis and receiving potentially curative therapy.

Mitochondria are important signaling and metabolic organelles that drive cells into apoptosis and they can also induce cellular proliferation. These biological functions are manipulated and processed by numerous proteins that are encoded in nuclear and mitochondrial genomes [5]. These proteins include mitofusin 1 and 2, which play a pivotal role in mitochondrial outer membrane fusion, and optic atrophy 1 (OPA1) which control the fusion of the inner mitochondrial membrane [6]. OPA1 is a large dynamin-like GTPase that promotes the fusion of mitochondria. OPA1 exists in two forms: long OPA1 (L-OPA1) and short OPA1 (S-OPA1). Two important proteases namely OMA1 and YME1 like 1 ATPase (YME1L) are involved in OPA-1 processing during cell cycle progression. OMA1 together with YME1L contributes to the hydrolysis of L-OPA1 into S-OPA1 [7]. Numerous mitochondrial proteins were found to be involved in proliferation and apoptosis in HCC. For example, downregulation of Opa1 mediated cell apoptosis by promoting mitochondrial fragmentation and mediating the release of cytochrome

[8]. Moreover, mitofusin 1 inhibited the proliferation and migration of HCC cells both *in vitro* and *in vivo* [9].

Disturbed mitochondrial proteases or mitochondrial respiratory deficiencies can provoke versatile signaling pathways that maintain the functional integrity of mitochondria [10]. OMA1 is present in the mitochondrial inner membrane. Proteolysis of OPA1 by OMA1 regulates both pro-survival and pro-apoptotic pathways [11]. The overexpression of OMA1 was reported in various cancers, including gastric cancer [12] and squamous cell lung carcinoma [13]. On the other hand, OMA1 overexpression enhances the overall survival of breast carcinoma [14]. The mitochondrial protein YME1L is also located in the inner mitochondrial membrane [15]. YME1L up-regulation is observed in different tumor cells, including non-small cell lung cancer (NSCLC) cells [16]. Previous studies illustrated that YME1L1 requires ATP for its activity while OMA1 is ATP-independent [17]. Therefore, it was suggested that both proteases degrade one another in a reciprocal process based on ATP levels [13]. Accordingly, OMA1 contribution to cancer progression is controversial. Moreover, the balance between the two proteases in different HCC stages is quite unclear. We therefore investigated the balance between OMA1/YME1L as a possible molecular target in HCC stages.

MATERIALS AND METHODS

Materials

Diethyl nitrosamine (DENA) with 99% purity was

obtained from Toronto Chemicals Co. (Canada) and phenobarbital sodium (PB) was purchased from Alpha-Chemika (India). Other used chemicals are of high quality and grade.

Animals

In the present study, 20 male albino rats (6 weeks) weighing 120 ± 20 grams were utilized. The sample size was calculated according to resource equation method [18], using the following formula: $E = \text{Total number of animals} - \text{Total number of groups}$, where the value of E should be in the range between 10 and 20 that considered as an adequate.

Animals were kept under standard conditions, including a temperature of $(25 \pm 2^\circ\text{C})$, 12 h light/dark cycle, and allowed free access to water and diet. The animal protocol was approved by the Ethical Committee in Kafrelsheikh University, Kafrelsheikh, Egypt, (approval code: KFS-IACUC/140/2023). All experiment was done at the animal house of Faculty of Pharmacy, Kafrelsheikh University, Kafrelsheikh, Egypt.

Experimental Design

Rats were acclimatized for 7 days and then were sorted randomly into four groups as the following:

Normal control group: Rats were intraperitoneally injected with saline (0.5-0.7 ml) and three DENA-treated groups: Rats received intraperitoneal injection of freshly prepared DENA (200 mg/kg, single dose). After 2 weeks from DENA administration, 0.05% of Pb was applied to their drinking water daily till the end of the experiment. Rats were then euthanized by inhalation with diethyl ether (sigma, USA) after 8, 16, and 24 weeks from DENA injection [19] (Figure 1) to obtain three stages of HCC.

Sample Collection

By the end of the experiment, blood samples were gathered from rats by puncturing the retroorbital venous plexus. The sera were then collected after blood centrifugation and kept frozen at -80°C for further biochemical investigation. Rats were then fasted for 12 hours to reduce variability in investigatory parameters and facilitating dissection of rats. They were then euthanized under anesthesia using diethyl ether (Sigma Aldrich, USA). The whole liver was then removed and divided into three portions. The first portion was immersed in phosphate-buffered formalin (pH 7.2, 10%) for histopathology and immunohistochemical investigation. The second one that was used for RT-PCR was immediately dipped in RNA later solution and then stored at -80°C . The third part was used to obtain liver homogenate in ice cold phosphate-buffered saline (PBS, pH 7.4). The liver homogenate samples were then stored at -80°C for western blot and

other biochemical analyses.

Histopathology of Liver Tissue

A neutral formalin solution (10%, pH=7.4) was used for liver specimen fixation. Ascending grades of ethanol were used for the dehydration of these specimens, which after that were embedded in paraffin wax to be sliced into sections of 5-7 μm thickness. Liver sections were then stained using hematoxylin and eosin (H&E) and were photographed and examined under a light microscope. Scoring of hepatic neoplastic lesion was done on the basis of the following criteria: nucleomegaly which graded from (0-4), necrosis graded from (0-4), mitosis which assessed as No/mm² and No and diameter of the preneoplastic foci.

Immunohistochemistry of Liver Specimens

Liver sections about 5 μm thick were deparaffinized using two xylene washes and rehydrated. Three percent Hydrogen peroxide and 1% bovine serum albumin were used for blocking endogenous peroxidase non-specific binding sites. After that, liver sections were incubated with anti-rat ki67 monoclonal antibody (1:200 dilution, Abcam Inc. Cat No. ab16667). They were also incubated with horseradish peroxidase conjugate anti-Rabbit antibody (Abcam Inc. Cat No. ab6721); 2% of 3,3 diamino-benzidine solution was utilized as a chromogen. Slides were counterstained using H&E. The percent of positive cells/1000 hepatocytes was then calculated.

Terminal Deoxynucleotidyl Transferase (TdT) dUTP-Nick-End Labeling (TUNEL) Assay

TUNEL assay was used for staining the apoptotic cells performing DNA fragmentation [20]. Liver sections are deparaffinized using two xylene washes, rinsing with descending concentrations of ethanol, and blocked. The slides were fixed by immersing them in freshly prepared 4% formaldehyde/PBS and washed in PBS solution. The slides were then covered with Proteinase K Solution, transferred into 4% formaldehyde/PBS, and washed in PBS. The slides were then stained with TUNEL according to the manufacturer's guidelines (BioVision, Milpitas, CA, USA). The positive apoptotic cells were counted per group in at least 10 fields.

Biochemical Analysis

Oxidative stress and lipid peroxidation were assessed in liver homogenate samples (each gram of liver tissue was homogenized in 10ml 50mM potassium phosphate, pH 7.5) by determining hepatic reduced glutathione (GSH) [21] and malondialdehyde (MDA) [22] contents (Biodiagnostic Co., Giza, Egypt).

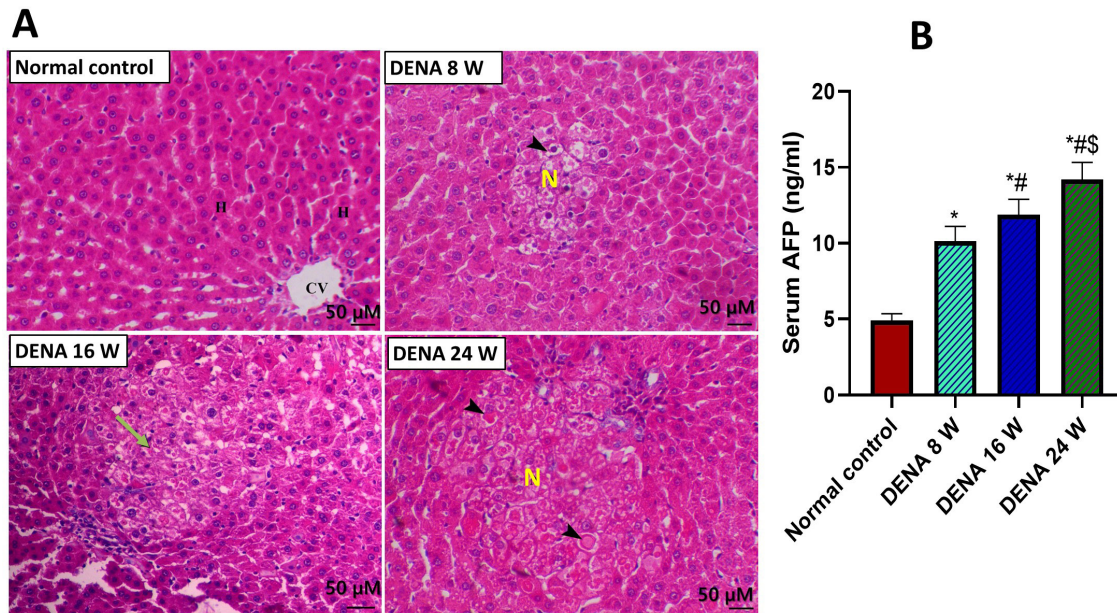


Figure 2. A. Representative micrographs of thin sections from liver samples of different studied rat groups showed normal hepatic architecture in the normal control group and dysplastic changes in the DENA treated groups. Bar=50 μM, H&E, X200. B. The serum alpha feto-protein (AFP) level in different studied rat groups. Data were expressed as mean±SD. * #, and \$ represent significant difference against normal control, DENA 8 W, and DENA 16 W, respectively.

Serum alpha-fetoprotein (AFP) was measured using the ELISA (enzyme-linked immunosorbent assay) technique (MyBioSource Co., USA, Cat no. MBS267612) [23] with a detection range of 0.312–20 ng/ml. Matrix metalloproteinase 9 (MMP 9) and cyclin D1 hepatic content were also detected in liver homogenate samples using the ELISA technique (MyBioSource Co., USA, Cat no. MBS722532, and LSF11068, respectively). The minimum limit of detection was up to 0.312–20 ng/ml for cyclin D1 and up to 0.1 ng/ml for MMP-9.

Western Blotting

RIPA lysis buffer (Himedia laboratories company, India) pretreated with phosphatase and proteinase inhibitor cocktail (Sigma-Aldrich, USA) was used for the preparation of liver homogenate samples (5 mg of the liver tissue from each sample was homogenized on ice with 300 μl of RIBA). Liver homogenate samples were then mixed with SDS-PAGE protein loading Buffer and boiled at 95°C. After that, protein samples were loaded onto SDS-PAGE gel (12%) and transferred to nitrocellulose membranes. After blocking with bovine serum albumin (3%), nitrocellulose membranes were incubated with primary antibodies (YME1L, TIMP-3 (dilution 1:1000, ABclonal company, USA) and OMA1 (dilution 1:1000, Thermo Fisher Scientific Inc, USA)) at 4°C overnight. Membranes were then washed and incubated with

horseradish peroxidase (HRP)– a conjugated secondary antibody (dilution: 1:2000, Abcam Inc., USA, Cat No. ab6721) at room temperature for 1.5 h. Western Bright enhanced chemiluminescence (ECL) HRP Substrate (Cat No. ab99697) was used for band detection. The intensity of the protein band was then detected using ImageJ software and normalized to β-actin (the housekeeping protein).

Real-time Polymerase Chain Reaction Analysis

RNA from tissues was isolated using TRIzol (Life Technologies, USA). The cDNA was then made according to the manufacturer's instructions of the RevertAid Synthesis Kit (Life Technologies). Quantitative real-time quantitative PCR analysis was then performed using A Maxima SYBR Green/Fluorescein master mix (Fermentas, USA) and cDNA samples as templates. 2–ΔΔ C T method was used to determine the fold change of target mRNA expression. The housekeeping gene (β-actin) was used for normalization. The used primers were:

Bax forward:5' CGGCGAATTGGAGATGAACTGG3' and reverse:5' CTAGCAAAGTAGAAGAGGGCAACC3'

TIMP-3 forward: 5'-GCCTTCTGCAACTCCGACATC-3' and reverse: 5'-CGTGTACATCTTGCCATCA-TA-3'

β-actin forward:5' -GATGGTGGGTATGGGT-

Table 1. Histopathological Scoring of Hepatic Neoplastic Features within the Different Examined Groups

Groups	Nucleomegaly Grade (0-4)	Mitosis No/mm ²	Necrosis Grade (0-4)	Preneoplastic foci No/mm ²	Diameter (μm)
Control	ND	ND	ND	ND	ND
DENA 8 W group	2.20±0.45	5.20±0.84	0.60±0.55	8.00±1.41	130.36±14.46
DENA 16 W group	3.20±0.45*	10.20±1.30*	1.40±0.55*	13.60±1.52*	278.98±18.70*
DENA 24 W group	3.80±0.45*#	16.80±1.30*#	2.20±0.45*#	23.40±1.14*#	711.49±47.73*#

Data are expressed as mean±SD, ND means non detectable lesion. * & # represent the significance against DENA 8-Week and DENA 16-Week groups respectively.

CAGAAGGAC-3' and reverse:5' -GCTCATTGCCGA-TAGTGATGACT-3'

Statistical Analysis

All data are expressed as mean values ± standard deviation (SD). ANOVA was used for multiple comparisons followed by Tukey posttest. Statistically significant was considered at $p < 0.05$. GraphPad Prism 8.0 (La Jolla, CA, USA) was used to perform the statistical analysis.

RESULTS

Histopathological Examination

As illustrated in Figure 2, the control animal showed normal hepatic parenchyma consisted of normal hepatocytes, normal arteriovenous, and sinusoidal blood vessels, and with normal biliary tissues. The induction of HCC demonstrated time-dependent manner of increase the neoplastic features within the hepatic tissues. The early neoplastic (DENA 8-week group) changes were demonstrated by presence of centrolobular hypertrophy of the hepatocytes, with small pandistributed foci of clear altered hepatic type. The liver of DENA 16-week group showed increase the size and number of preneoplastic foci with marked increase the eosinophilic and mixed type. The hepatocytes within the foci showed marked nucleomegaly, increases mitotic figures, central necrosis as well as marked thickening of the hepatic plates and oval cells hyperplasia. The DENA 24-week group showed marked increase of these hepatic dysplastic features with cytoplasmic inclusions and remarkable increase the size and number of the preneoplastic foci. The neoplastic criteria were graded in a quantitative score and mentioned in Table 1.

Serum AFP Level

Serum AFP is routinely used as an HCC tumor marker for diagnosis, screening, and follow-up treatment. HCC is usually associated with elevated serum AFP levels [24]. Previous study also reported that AFP was useful for de-

tecting a molecular subclass of HCC as its concentration increased in different HCC groups that stratified based different parameters including tumor size and degree of cellular differentiation [25]. Other study also demonstrated that the DENA-treated groups displayed a significant increase ($p < 0.001$) in AFP at the end of 6, 9, 12, 15, 18, 21, 24, and 27 weeks, compared with their corresponding values in the control groups [26]. Here, the current study revealed a significant elevation in the serum AFP level in DENA 8 W group compared to the normal control one. The serum AFP level also exhibited a significant increase in the DENA 16 W compared to the DENA 8 W group and much increase in the DENA 24 W Figure 2B.

The Hepatic Expression of Mitochondrial Proteins OMA1 and YME1L

The hepatic expression of two inner mitochondrial proteins (YME1L and OMA1) was assessed using the western blot technique. Our results showed that the hepatic expression of OMA1 protein was significantly decreased in the DENA-treated groups, compared to the normal one. Its expression was significantly decreased in the DENA 16 W and much decreased in the DENA 24 W group (Figure 3A). On the other hand, the hepatic expression of YME1L protein was significantly increased in the DENA-treated groups, compared to the normal one, and its expression was significantly increased in the DENA 16 W and much elevated in the DENA 24 W group (Figure 3B).

The Assessment of the Hepatic Apoptosis

Bax is a main regulator of cell death and is an important gateway to mitochondrial dysfunction. It is a chief pro-apoptotic protein of the Bcl-2 family and controls apoptosis in normal and tumor cells. One of the main mechanisms of tumorigenesis is apoptosis dysfunction [27]. To evaluate the role of the mitochondrial proteins OMA1 and YME1L on apoptosis, the hepatic expression of the apoptotic marker *Bax* mRNA was assessed using RT-PCR, and the percent of apoptotic cells was also calculated in different groups using TUNEL assay (Fig-

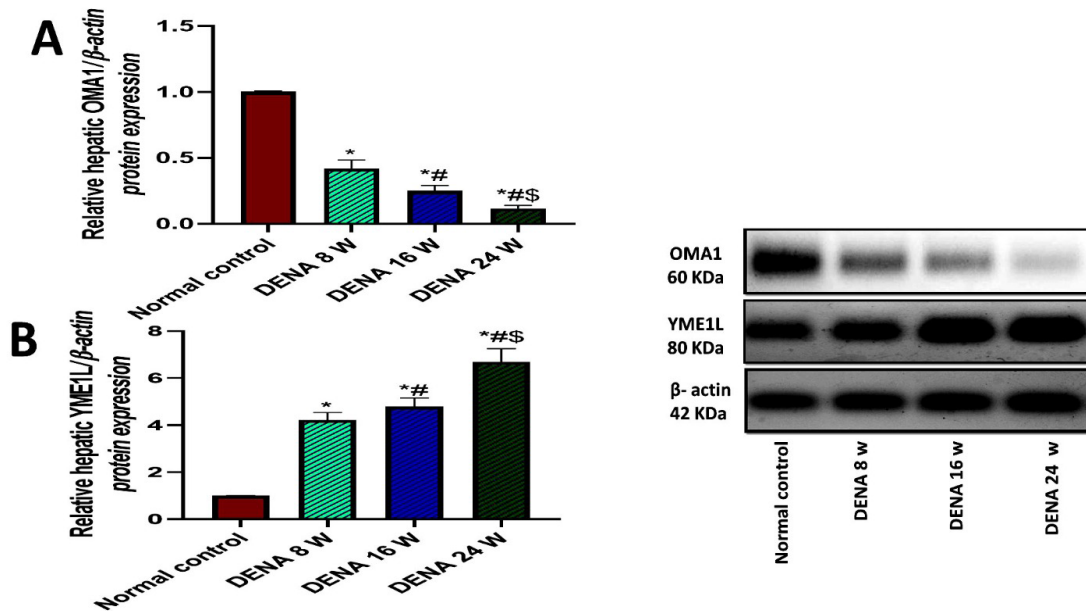


Figure 3. The relative hepatic protein expression of (A) OMA1 and (B) YME1L/ β -actin in different studied rat groups. Data were expressed as mean \pm SD. *, #, and \$ represent significant difference against normal control, DENA 8 W, and DENA 16 W, respectively.

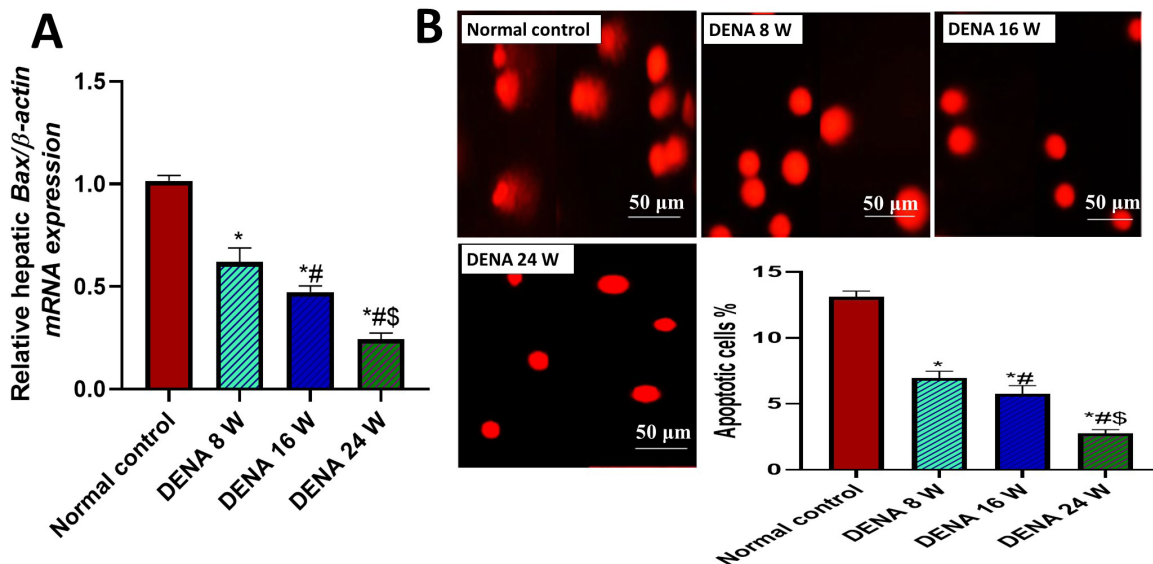


Figure 4. A. The relative hepatic Bax/ β -actin mRNA expression in different studied rat groups. B. The percent of apoptotic cells in hepatic tissues of different groups that were measured using TUNEL assay. Data were expressed as mean \pm SD. *, #, and \$ represent significant difference against normal control, DENA 8 W, and DENA 16 W, respectively. bar 50 μ m.

ure 4). The present study displayed that DENA-treated groups showed a significant decrease in apoptosis, which appeared in a marked reduction in the relative expression of the pro-apoptotic marker *Bax* (Figure 4A) and a decrease in the percent of apoptotic cells (Figure 4B), compared to the normal control group. These static apoptotic variations increased in the DENA 16 W group and much increased in the DENA 24 W group, compared to the normal control group (Figure 4).

The Evaluation of the Hepatic Cell Cycle Arrest and Cellular Proliferation

Cell cycle arrest was assessed by measuring the concentration of cyclin D1, which is considered the main cell cycle regulator. Cyclin D1 contributes to cancer pathogenesis as it causes uncontrolled cellular proliferation. The expression of cyclin D1 is strictly regulated in normal cells. Conversely, its activity is markedly elevated in cancer [28]. Our study revealed that the level of cyclin D1 is markedly elevated in all DENA-treated groups, in comparison to the normal control one. Additionally, its level is significantly increased in DENA 24 W compared to DENA 8 W and 16 W groups. However, no significant difference was observed between DENA 8 W and 16 W groups (Figure 5A).

Antigen Ki-67, a nuclear protein, is expressed in proliferating cells of mammalian and commonly used as proliferating marker in cancer histopathology [29]. Our study revealed that negative staining of the Ki-67 was noticed in the normal control group. However, the Ki-67 was observed as a positive brown nuclear expression in hepatocytes in DENA 8 W group that elevated in DENA 16 W group and much more increased in DENA 24 W group (Figure 5B).

The Assessment of the Hepatic Metastatic Markers

Matrix metalloproteinases (MMPs) are a family of zinc-dependent endopeptidases. They play a vital role in the remodeling of extracellular matrix in cancer development and progression. One member of this family is MMP9, which acts as a chief mediator in metastatic progression [30]. Members of the MMP family are inhibited by tissue inhibitors of matrix metalloproteinases (TIMPs). The invasiveness of cancer cells depends on the balance between MMPs and TIMPs. The major tissue inhibitor of MMP-9 is TIMP-3, which controls the invasion [31].

The current study revealed that all DENA-treated groups showed a significant increase in the hepatic concentration of MMP-9 and in parallel, a marked decrease in the hepatic expression of its inhibitor TIMP-3 mRNA and protein, compared with the normal control group. It was also noticed a more significant variation in the pre-

vious metastatic parameters in the DENA 24 W group, compared to the DENA 8 W and 16 W groups (Figure 6A-C).

Variations in Oxidative Stress in Hepatic Tissue Homogenate of Different Rat Groups

To assess the oxidative stress variations in the hepatic tissue of different rat groups, malondialdehyde (MDA), and reduced glutathione (GSH) were measured spectrophotometry. MDA mediates carcinogenesis by inducing alterations of DNA [32]. On the other hand, GSH protects against reactive oxygen species (ROS) so its concentration decreased in cancer tissues [33]. The current study exhibited a marked increase in the hepatic content of MDA and a significant decline in the GSH level in the DENA treated groups, in contrast to the normal control one. Additionally, these variations showed a significant increase as the stage of HCC increased (Figure 7 A-B).

Correlations between OMA1, YME1L, and AFP

Lastly, we also assessed possible correlations between the hepatic expression of (OMA1 and YME1L) and the liver tumor marker AFP and between the hepatic expression of OMA1 and YME1L. It can be observed in Figure 8 A-C that OMA1 was inversely correlated with AFP ($r = -0.9272$; $p = 0.023$) and YME1L ($r = -0.9748$; $p = 0.0048$). There was also a positive correlation between YME1L and AFP ($r = 0.8058$; $p = 0.0387$).

DISCUSSION

HCC is considered the fifth most frequent cancer globally and is characterized by poor prognosis due to the late diagnosis at advanced stages of tumor development. Accordingly, the identification of novel early-stage biomarkers for HCC results in significant benefits including early screening and treatment [34]. Facts about molecular mechanisms of HCC development and progression remain unclear. Therefore, there is an urgent need for more in-depth understanding of these mechanisms, which also help in identifying novel biomarkers for HCC diagnosis [35]. One of these mechanisms that contribute to HCC development is mitochondrial dysfunction.

Mitochondria are vital organelles that can mediate cancer development in numerous biological aspects, involving bioenergetics metabolism, biosynthetic, signaling, oxidative stress, and regulation of cell death [36]. OMA1 and YME1L, the mitochondrial inner membrane proteases, are important regulators of crucial mitochondrial functions including mitochondrial dynamics and proteases maintenance of the mitochondrial inner membrane [37]. In the present study, we illustrated that the role of OMA1 and YME1L in hepatocarcinogenesis in

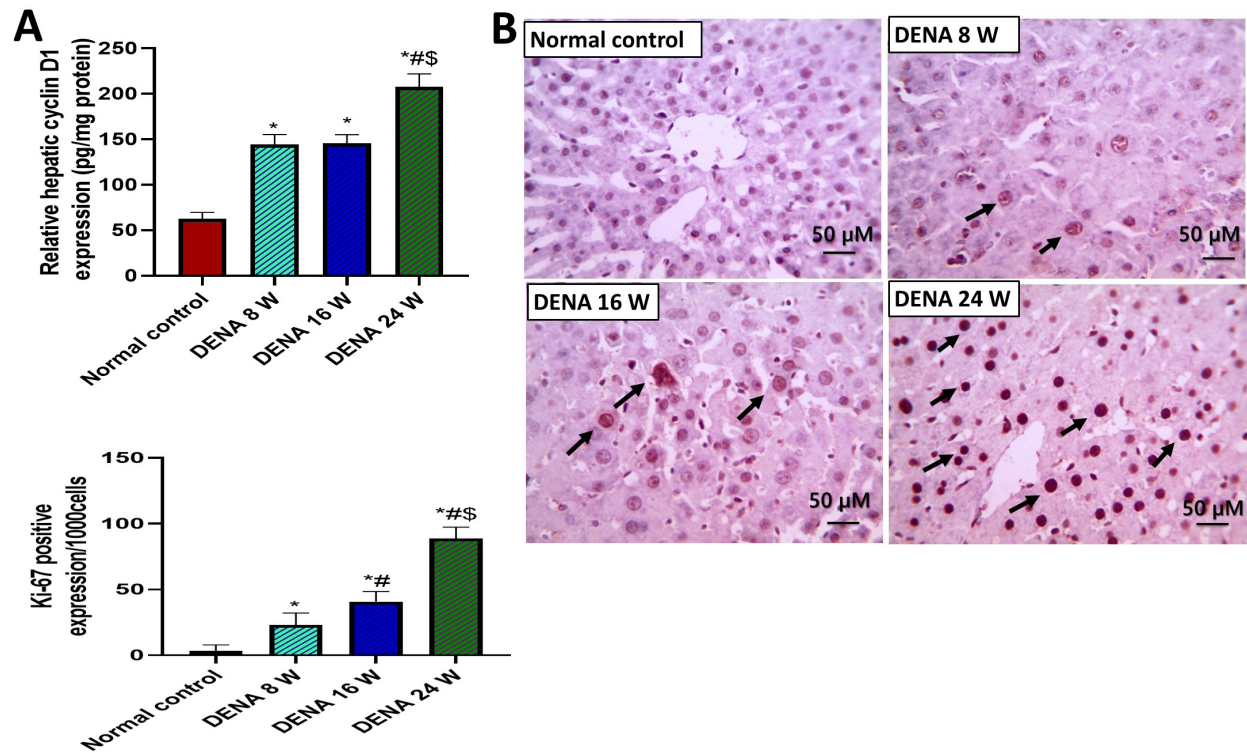


Figure 5. The relative hepatic expression of (A) cyclin D1 protein (pg/mg protein) and (B) Ki-67 in various rat groups. Data were expressed as mean \pm SD. *, #, and \$ represent significant difference against normal control, DENA 8W, and DENA 16 W, respectively. X:400 bar 50 μ m.

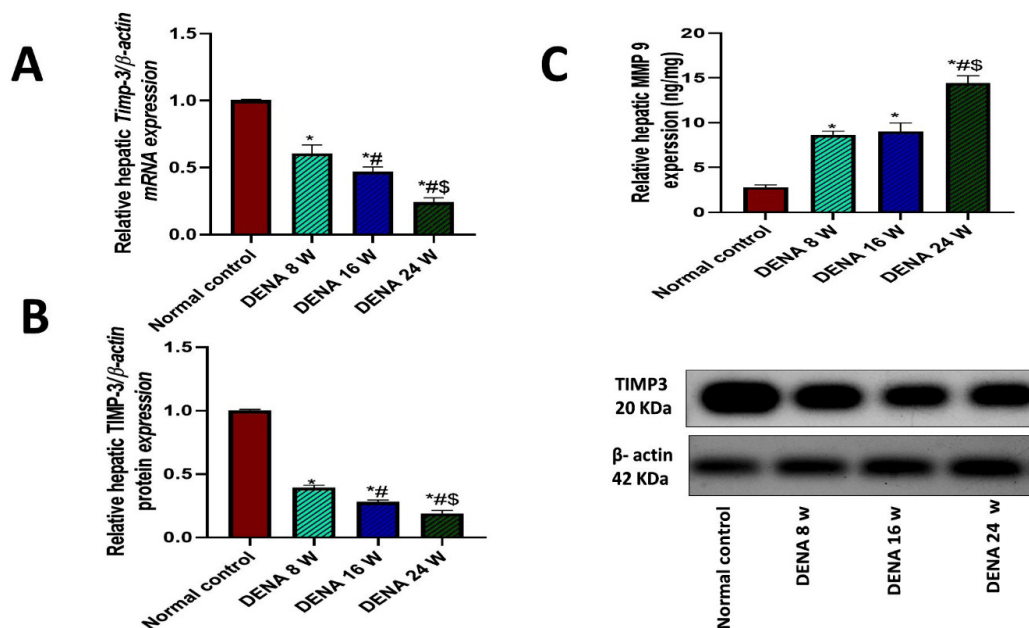


Figure 6. The relative hepatic expression of (A) the hepatic expression of tissue inhibitor matrix metalloproteinase-3 (TIMP-3) mRNA (B) TIMP-3 protein expression and (C) hepatic matrix metalloproteinase 9 (mmp9) content in different rat groups. Data were expressed as mean \pm SD. *, #, and \$ represent significant difference against normal control, DENA 8 W, and DENA 16 W, respectively.

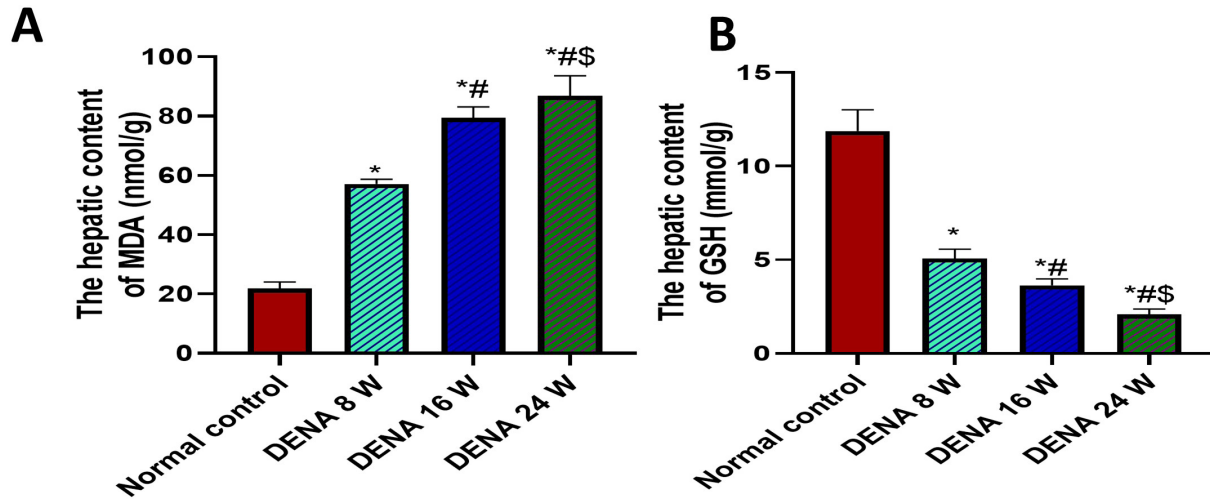


Figure 7. The hepatic content of (A) MDA and (B) GSH in liver homogenate of different groups. DENA: diethyl nitrosamine, GSH: reduced glutathione, MDA; malonaldehyde. Data were expressed as mean \pm SD. *, #, and \$ represent significant difference against normal control, DENA 8 W, and DENA 16 W, respectively.

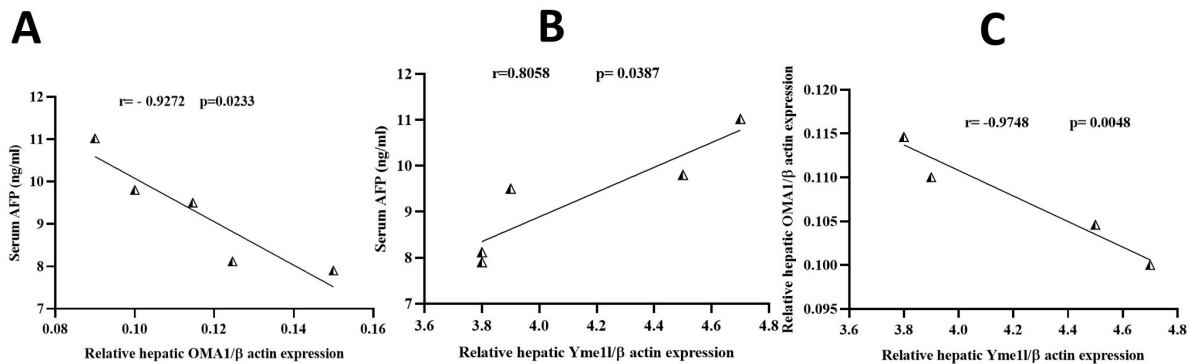


Figure 8. Correlation between the serum level of AFP versus (A) OMA1 (B) YME1L hepatic expression and between the hepatic expression of YME1L and OMA1. Graphs show the Pearson correlation coefficient and probabilities.

the experimental rat model.

Two mitochondrial proteases, OMA1 and YME1L, exist in the inner mitochondrial membrane (IMM) and play an important role in several mitochondrial processes, including maintaining mitochondrial morphology, plasticity, as well as function [38]. Accordingly, imbalances in the activity of OMA1 and YME1L may contribute to carcinogenesis. To investigate their role in hepatocarcinogenesis, their protein expression was assessed in different stages of chemically-induced HCC in rats. HCC induction was confirmed by histopathological examination of liver tissue and via measuring serum AFP in different rat group samples. Our findings revealed for the first time that OMA1 protein expression is down-regulated in the

hepatic tissues of HCC groups, while YME1L is up-regulated in HCC. More interestingly, the expression of both molecules was significantly different among HCC stages. However, the study of the gene level of these proteins and other genes that may change protein expression should be considered.

It has been reported that OMA1 was down-regulated in breast cancer and this downregulated expression was associated with disturbed proliferative properties of cancer cells [14]. Conversely, OMA1 was overexpressed in colorectal cancer by the metabolic reprogramming under hypoxia [39]. *Oma1* gene expression was also significantly increased in gastric cancer tissue compared to healthy adjacent tissue [12]. These may refer to the differential

expression of OMA1 among cancer types. Our previous data reported that the hepatic expression of YME1L is significantly increased in HCC tissues compared to the healthy ones [7]. The expression of YME1L was also increased in different cancer types including non-small cell lung cancer [40] and glioma cells [41].

Additionally, YME1L and OMA1 expressions and function are highly responsive to stress conditions including oxidative stress. Oxidative stress could modulate the proteolytic activity of YME1L and OMA1 to OPA1. Inducing oxidative stress with adequate ATP level may result in OMA1 degradation and enhancing YME1L function [42]. Our study revealed an elevated oxidative stress levels in HCC tissues compared to healthy tissues as evidenced by increased MDA and decrease GSH. Hence, the tumor microenvironment with high oxidative stress levels may explain the up-regulation of YME1L and downregulation of OMA1. Moreover, it is reported that downregulation of OMA1 may be responsible for increased ROS production [43].

For further explanation of the possible diagnostic role of OMA1/YME1L panel, this study tried to investigate the effect of these molecules on the biological behavior of cells including apoptosis and proliferation. Our data revealed that the hepatic expression of *Bax* was significantly decreased in different cancer stages with lower OMA1 expression and higher YME1L up-regulation compared to the normal tissues. Of note, the hepatic expression of OMA1 and YME1L and *Bax* was stage-dependent. These results were further confirmed using TUNEL assay, where decreased percentage of apoptotic cells was evidenced in tumor tissues compared to normal one.

Consistent with our data, YME1L has been identified as a regulator of cell apoptosis and proliferation in different tumor cells including NSCLC cells where depletion of YME1L promotes NSCLC cells apoptosis [16]. On the other hand, the inactivation of OMA1 in tumor tissues may be associated with down-regulation of BCL2/*Bax* signaling pathway. It has been reported that apoptosis is induced by aggregation of the *Bax* protein on the surface of mitochondria. Upon *Bax* aggregation, OMA1 is activated resulting in cleaving of OPA1. The OPA1 cleavage promotes mitochondrial cristae remodeling, inducing the release of the majority of cytochrome *c* inside the cristae, which ultimately triggers apoptosis [44]. Hence, down-regulation of BCL2/*Bax* signaling pathway in different stages of HCC may clarify the down-regulation of OMA1 in different HCC stages.

Our results showed a potential role of YME1L in cell proliferation and consequently cell survival. Our study revealed that the cell proliferative marker, Ki-67, and cell cycle arrest marker, cyclin D1, were markedly elevated in tumor tissues that exhibiting low hepatic OMA1 protein expression and high YME1L compared to normal

tissues. In supporting of these results, a previous study reported that the expression of Ki-67 was higher in *in vitro* breast cancer cells with OMA1 silencing, compared to normal cells [14]. Furthermore, the proliferative effect of YME1L1 was previously discussed in ovarian cancer. Liao and colleagues pointed out that YME1L1 is up-regulated in ovarian cancer tissues compared to normal tissues [5]. Of note, this high expression was reported in ovarian cancer patients with advanced stages and it was associated with tumor progression [16].

These results evoke a question about the YME1L/OMA1 expression and disease progression. So, we evaluated the expression of metastatic markers in hepatic tissues. The metastatic marker MMP-9 was significantly elevated in the tumor tissues with low OMA1 and high YME1L expression compared to the normal ones. On the other hand, HCC tissues in different stages displayed a significant decrease in the hepatic TIMP-3 (a MMP-9 inhibitor) gene expression, compared to normal cells. This agreed with previous studies reported that deletion of OMA1 promotes the malignant progression of breast cancer cells [14] and YME1L expression was highly expressed in late stage ovarian cancer patients [5].

Hence, the main finding of this study is the up-regulation of YME1L and down-regulation of OMA1 in HCC, compared to normal tissues. The reported expression of these proteases was associated with anti-apoptotic activity as evidenced by *Bax* expression and TUNEL assay. These molecules were also associated with cell proliferation as reflected from Ki-67 expression and histopathological examination of hepatic tissues. More interestingly, these molecular events appeared in early stages of HCC and increase significantly with various HCC stages. There is a paucity of data about the role of this panel in different neoplastic stages whether in animal model or clinical studies. Our results recommend YME1L/OMA1 panel as possible diagnostic tool that may have some benefits in early diagnosis; however, more studies are needed to confirm these finding in human tissues and assess modulator of these proteases as a possible therapeutic agent in HCC.

Institutional Review Board Statement: The animal protocol was approved by the Ethical Committee in the Faculty of Pharmacy, Kafrelsheikh University, Kafrelsheikh, Egypt, (approval code: KFS-IACUC/140/2023).

Informed Consent Statement: Not applicable.

Data Availability Statement: Data will be made available upon request.

Conflicts of Interest: The authors declare no conflict of interest.

Funding: This research received no external funding.

REFERENCES

1. Ganesan P, Kulik LM. Hepatocellular Carcinoma: new De-

- velopments. *Clin Liver Dis*. 2023 Feb;27(1):85–102.
2. Lin D, Luo R, Ye Z, Wei Q, Bae H, Juon HS, et al. Genomic characterization of early-stage hepatocellular carcinoma patients with Hepatitis B using circulating tumor DNA. *Clin Res Hepatol Gastroenterol*. 2023 Aug;47(7):102161.
 3. Farinati F, Marino D, De Giorgio M, Baldan A, Cantarini M, Cursaro C, et al. Diagnostic and prognostic role of α -feto-protein in hepatocellular carcinoma: both or neither? *Official journal of the American College of Gastroenterology|ACG*. 2006;101(3):524–32. <https://doi.org/10.1111/j.1572-0241.2006.00443.x>.
 4. Pinto A, Pinto F, Faggian A, Rubini G, Caranci F, Macarini L, et al. Sources of error in emergency ultrasonography. *Critical ultrasound journal*. 2013;5 Suppl 1(Suppl 1):S1. *Epub* 2013/08/02. <https://doi.org/10.1186/2036-7902-5-S1-S1>.
 5. Liao WT, Chu PY, Su CC, Wu CC, Li CJ. Mitochondrial AAA protease gene associated with immune infiltration is a prognostic biomarker in human ovarian cancer. *Pathol Res Pract*. 2022 Dec;240:154215.
 6. Yapa NM, Lisnyak V, Reljic B, Ryan MT. Mitochondrial dynamics in health and disease. *FEBS Lett*. 2021 Apr;595(8):1184–204.
 7. Mohie Abdel-Hamid N, Abass SA, Eldomany R. Assessment of YME1L and mitofusin2 as a possible diagnostic and/or therapeutic target in hepatocellular carcinoma [IJBB]. *Indian J Biochem Biophys*. 2022;60(1):43–54.
 8. Zhao X, Tian C, Puszyk WM, Ogunwobi OO, Cao M, Wang T, et al. OPA1 downregulation is involved in sorafenib-induced apoptosis in hepatocellular carcinoma. *Lab Invest*. 2013 Jan;93(1):8–19.
 9. Zhang Z, Li TE, Chen M, Xu D, Zhu Y, Hu BY, et al. MFN1-dependent alteration of mitochondrial dynamics drives hepatocellular carcinoma metastasis by glucose metabolic reprogramming. *Br J Cancer*. 2020 Jan;122(2):209–20.
 10. Song J, Herrmann JM, Becker T. Quality control of the mitochondrial proteome. *Nat Rev Mol Cell Biol*. 2021 Jan;22(1):54–70.
 11. Murata D, Yamada T, Tokuyama T, Arai K, Quirós PM, López-Otin C, et al. Mitochondrial Safeguard: a stress response that offsets extreme fusion and protects respiratory function via flickering-induced Oma1 activation. *EMBO J*. 2020 Dec;39(24):e105074.
 12. Amini MA, Karimi J, Khodadadi I, Tavilani H, Talebi SS, Afshar B. Overexpression of ROMO1 and OMA1 are potentially biomarkers and predict unfavorable prognosis in gastric cancer. *J Gastrointest Cancer*. 2020 Sep;51(3):939–46.
 13. Alavi MV. Targeted OMA1 therapies for cancer. *Int J Cancer*. 2019 Nov;145(9):2330–41.
 14. Daverey A, Levtytsky RM, Stanke KM, Viana MP, Swenson S, Hayward SL, et al. Depletion of mitochondrial protease OMA1 alters proliferative properties and promotes metastatic growth of breast cancer cells. *Sci Rep*. 2019 Oct;9(1):14746.
 15. Hartmann B, Wai T, Hu H, MacVicar T, Musante L, Fischer-Zirnsak B, et al. Homozygous YME1L1 mutation causes mitochondriopathy with optic atrophy and mitochondrial network fragmentation. *eLife*. 2016 Aug;5:e16078.
 16. Xia Y, He C, Hu Z, Wu Z, Hui Y, Liu YY, et al. The mitochondrial protein YME1 Like 1 is important for non-small cell lung cancer cell growth. *Int J Biol Sci*. 2023 Mar;19(6):1778–90.
 17. Kaser M, Kambacheld M, Kisters-Woike B, Langer T. Oma1, a novel membrane-bound metalloproteinase in mitochondria with activities overlapping with the m-AAA protease. *J Biol Chem*. 2003 Nov;278(47):46414–23.
 18. Charan J, Kantharia ND. How to calculate sample size in animal studies? *J Pharmacol Pharmacother*. 2013 Oct;4(4):303–6.
 19. Abdel-Hamid NM, Zakaria SM, Ansary AM, El-Senduny FF, El-Shishtawy MM. The expression of tuftelin 1 as a new theranostic marker in early diagnosis and as a therapeutic target in hepatocellular carcinoma. *Cell Biochemistry and Function*. <https://doi.org/10.1002/cbf.3828>.
 20. Gavrieli Y, Sherman Y, Ben-Sasson SA. Identification of programmed cell death in situ via specific labeling of nuclear DNA fragmentation. *J Cell Biol*. 1992 Nov;119(3):493–501.
 21. Beutler E, Duron O, Kelly BM. Improved method for the determination of blood glutathione. *The Journal of laboratory and clinical medicine*. 1963;61:882–8.
 22. Ohkawa H, Ohishi N, Yagi K. Assay for lipid peroxides in animal tissues by thiobarbituric acid reaction. *Anal Biochem*. 1979 Jun;95(2):351–8.
 23. Cattini R, Cooksey M, Robinson D, Brett G, Bacarese-Hamilton T, Jolley N. Measurement of α -Fetoprotein, Carcinoembryonic Antigen and Prostate-Specific Antigen in Serum and Heparinised Plasma by Enzyme Immunoassay on the Fully Automated Serono SR1™ Analyzer. *Eur J Clin Chem Clin Biochem*. 1993;31(8):517–24. <https://doi.org/10.1515/cclm.1993.31.8.517>.
 24. Lee CW, Tsai HI, Lee WC, Huang SW, Lin CY, Hsieh YC, et al. Normal alpha-fetoprotein hepatocellular carcinoma: are they really normal? *J Clin Med*. 2019 Oct;8(10):1736.
 25. Galle PR, Foerster F, Kudo M, Chan SL, Llovet JM, Qin S, et al. Biology and significance of alpha-fetoprotein in hepatocellular carcinoma. *Liver Int*. 2019 Dec;39(12):2214–29.
 26. Fathy AH, Bashandy MA, Bashandy SA, Mansour AM, Elsadek B. Sequential analysis and staging of a diethylnitrosamine-induced hepatocellular carcinoma in male Wistar albino rat model. *Can J Physiol Pharmacol*. 2017 Dec;95(12):1462–72.
 27. Liu Z, Ding Y, Ye N, Wild C, Chen H, Zhou J. Direct Activation of Bax Protein for Cancer Therapy. *Med Res Rev*. 2016 Mar;36(2):313–41.
 28. Montalto FI, De Amicis F. Cyclin D1 in Cancer: A Molecular Connection for Cell Cycle Control, Adhesion and Invasion in Tumor and Stroma. *Cells*. 2020 Dec;9(12):2648.
 29. Sobocki M, Mrouj K, Camasses A, Parisi N, Nicolas E, Llères D, et al. The cell proliferation antigen Ki-67 organizes heterochromatin. *eLife*. 2016 Mar;5:e13722.
 30. Owyong M, Chou J, van den Bijgaart RJ, Kong N, Efe G, Maynard C, et al. MMP9 modulates the metastatic cascade and immune landscape for breast cancer anti-metastatic therapy. *Life Sci Alliance*. 2019 Nov;2(6):e201800226.
 31. Jiang G, Qi Y. Detection of MMP-9 and TIMP-3 mRNA expression in the villi of patients undergoing early spontaneous abortion: A report of 30 cases. *Exp Ther Med*. 2015

- May;9(5):1939–43.
32. Abdel-Hamid NM, Mahmoud TK, Abass SA, El-Shishtawy MM. Expression of thioredoxin and glutaredoxin in experimental hepatocellular carcinoma-Relevance for prognostic and diagnostic evaluation. *Pathophysiology : the official journal of the International Society for Pathophysiology*. 2018;25(4):433-8. Epub 2018/09/19. <https://doi.org/10.1016/j.pathophys.2018.08.008>.
 33. Czczot H, Scibior D, Skrzycki M, Podsiad M. Glutathione and GSH-dependent enzymes in patients with liver cirrhosis and hepatocellular carcinoma. *Acta Biochim Pol*. 2006;53(1):237–42.
 34. Tsuchiya N, Sawada Y, Endo I, Saito K, Uemura Y, Nakatsura T. Biomarkers for the early diagnosis of hepatocellular carcinoma. *World J Gastroenterol*. 2015 Oct;21(37):10573–83.
 35. Ogunwobi OO, Harricharran T, Huaman J, Galuza A, Odumuwagon O, Tan Y, et al. Mechanisms of hepatocellular carcinoma progression. *World J Gastroenterol*. 2019 May;25(19):2279–93.
 36. Vyas S, Zaganjor E, Haigis MC. Mitochondria and Cancer. *Cell*. 2016 Jul;166(3):555–66.
 37. Rainbolt TK, Lebeau J, Puchades C, Wiseman RL. Reciprocal degradation of YME1L and OMA1 adapts mitochondrial proteolytic activity during stress. *Cell Rep*. 2016 Mar;14(9):2041–9.
 38. Ohba Y, MacVicar T, Langer T. Regulation of mitochondrial plasticity by the i-AAA protease YME1L. *Biol Chem*. 2020 May;401(6-7):877–90.
 39. Wu Z, Zuo M, Zeng L, Cui K, Liu B, Yan C, et al. OMA1 reprograms metabolism under hypoxia to promote colorectal cancer development. *EMBO Rep*. 2021 Jan;22(1):e50827.
 40. Xia Y, He C, Hu Z, Wu Z, Hui Y, Liu YY, et al. The mitochondrial protein YME1 Like 1 is important for non-small cell lung cancer cell growth. *Int J Biol Sci*. 2023 Mar;19(6):1778–90.
 41. Liu F, Chen G, Zhou LN, Wang Y, Zhang ZQ, Qin X, et al. YME1L overexpression exerts pro-tumorigenic activity in glioma by promoting Gαi1 expression and Akt activation. *Protein Cell*. 2023 Apr;14(3):223–9.
 42. Murphy MP. How mitochondria produce reactive oxygen species. *Biochem J*. 2009 Jan;417(1):1–13.
 43. Miallot R, Millet V, Groult Y, Modelska A, Crescence L, Roulland S, et al. An OMA1 redox site controls mitochondrial homeostasis, sarcoma growth, and immunogenicity. *Life Sci Alliance*. 2023 Apr;6(6):e202201767.
 44. Jiang X, Jiang H, Shen Z, Wang X. Activation of mitochondrial protease OMA1 by Bax and Bak promotes cytochrome c release during apoptosis. *Proc Natl Acad Sci USA*. 2014 Oct;111(41):14782–7.